ELSEVIER

Polymer 44 (2003) 2529–2536

polymer

www.elsevier.com/locate/polymer

Aggregation behavior of two-arm fullerene-containing poly(ethylene oxide)

T. Song[a], S. Dai[b], K.C. Tam[b,*], S.Y. Lee[a], S.H. Goh[a,*]

[a]*Department of Chemistry, National University of Singapore, 3 Science Drive 3, Singapore 117543, Singapore*
[b]*School of Mechanical and Production Engineering, Nanyang Technological University, 50 Nanyang Avenue, Singapore 639798, Singapore*

Received 10 September 2002; received in revised form 18 December 2002; accepted 20 January 2003

Abstract

A water-soluble two-arm fullerene-containing poly(ethylene oxide) (PEO) was synthesized through isocyanate-hydroxy condensation reaction with fullerenol as a molecular core and characterized by Fourier transform infrared spectroscopy, X-ray photoelectron spectroscopy, thermogravimetry, and matrix-assisted laser desorption ionization time of flight mass spectrometry. The aggregation behavior of the resulting amphiphilic polymer in water, THF, and DMF, was studied by gel permeation chromatography, laser light scattering, and transmission electron microscopy. The polymer forms spherical aggregates with an aggregation number around 540–1020.

Keywords: Poly(ethylene oxide); Aggregation behavior; Fullerene

1. Introduction

[60]Fullerene, C_{60}, has attracted much attention due to its unique chemical and physical properties [1]. However, its poor solubility and processability pose difficulties in practical applications. Grafting polymer chains on fullerene is gaining particular interest because a combination of fullerene and polymer not only significantly improves the solubility and processability of fullerene but also leads to useful materials. Various kinds of C_{60}-containing polymers have been synthesized, but their solubility behavior in organic solvents has mainly been focused on a few C_{60}-containing polymers, such as C_{60}-containing polystyrene (PS), poly(*p*-vinylphenol) (PVPh), poly(methyl methacrylate) (PMMA) and poly(*n*-butyl methacrylate) (PBMA) [2–10]. A static laser light-scattering (LLS) study showed that fullerene grafted with two well-defined PS or PVPh arms could form micelles in tetrahydrofuran (THF) [5]. A combination of static and dynamic LLS studies revealed that micelle-like core–shell aggregates with C_{60} as the core and polymer chains as the shell exist in C_{60}-containing PMMA and PBMA in THF solutions [8]. However, the formation of aggregates and the control of the aggregation size have important implications for the fullerene application in the field of nonlinear optical systems and in the biomedical area.

Recently, Zhou et al. studied the association behavior of a fullerene derivative, the potassium salt of pentaphenyl fullerene, in water by LLS [11]. The average aggregation number of associated particles in the large spherical vesicles is about 1.2×10^4. Moreover, they expected that C_{60}-based 'surfactants' may be synthesized through versatile organic chemistry designs to form a vesicle-membrane system as an alternative to lipid membranes and liposome vesicles in biology and medicine applications. Instead of the flexible hydrophobic tails, the modified C_{60} has a rigid hydrophobic ball with a dominant intrinsic geometric constraint. Samal and Geckeler also used LLS to study cluster–cluster aggregation phenomena in aqueous solutions of fullerene–cyclodextrin conjugates, and found that the average particle size increases from 0.55 to 3.255 μm with decreasing concentration of the solution [12]. The aggregation of an amphiphilic C_{60}-derivative (*R*)-2-acetyl-carnitine(5-(fulleropyrrolidin-1-yl)-3-oxapentan-1-yl) ester (AFE) in aqueous solution, determined by static light scattering (SLS) and reversed-phase chromatography experiments, suggested an average diameter of 120 nm for the aggregates [13].

* Corresponding authors. Tel.: +65-6790-5590; fax: +65-6791-1859 (K.C. Tam). Tel.: +65-6874-2844; fax: +65-6779-1691 (S.H. Goh).
E-mail addresses: mkctam@ntu.edu.sg (K.C. Tam), chmgohsh@nus.edu.sg (S.H. Goh).

0032-3861/03/$ - see front matter © 2003 Elsevier Science Ltd. All rights reserved.
doi:10.1016/S0032-3861(03)00107-1

Poly(ethylene oxide) (PEO) is well known not only for its relatively simple structure but also for its remarkable biomedical properties. The grafting of such a biocompatible polymer onto C_{60} is of special interest since the importance of the fullerene molecule in the biomedical and biotechnological fields has been established. Poly(ethylene oxide)-modified fullerenes have been prepared with a precursor PEO possessing mono- or di-azido end-groups [14–16]. C_{60}-containing PEOs were also synthesized from mono- or di-amino terminated PEO [17,18]. 'Living' PEO, such as PEO-K^+, can be grafted onto C_{60} [19,20]. Interestingly, the aggregation of such C_{60}-containing PEO in THF was observed by gel permeation chromatography (GPC) [19,20].

Polyhydroxylated C_{60} derivative (fullerenol) is a versatile intermediate in the design of C_{60}-containing polymers [21,22]. In this study, mono-isocyanate terminated PEO was reacted with fullerenol to afford a urethane-connected C_{60}-containing PEO. The resulting PEO was found to predominantly contain two covalently bonded polymer arms per C_{60}, based on Fourier transform infrared spectroscopy (FTIR), X-ray photoelectron spectroscopy (XPS), thermogravimetry (TG), and matrix-assisted laser desorption ionization time of flight mass spectrometry (MALDI-TOF). Large aggregates were found to form in solutions as shown by GPC, LLS, and transmission electron microscopy (TEM).

2. Experimental

2.1. Materials and sample preparation

C_{60} (99.9% pure) was obtained from Peking University, China. Fullerenol was synthesized following the published method [23]. Poly(ethylene glycol) monomethyl ether (MPEO) was obtained from Aldrich; its number-average molecular weight (M_n) and polydispersity are 2050 and 1.06, respectively, as determined by MALDI-TOF mass spectrometry. Residual water in the sample was removed by azeotropic distillation with toluene. Hexamethylene diisocyanate (HDI) and dibutyltin dilaurate were obtained from Merck. Anhydrous *N*,*N*′-dimethylformamide (DMF) was prepared by distillation under a reduced pressure and stored over molecular sieves (4 Å). Other solvents were of analytical pure grade and were used as received. The standard poly(ethylene oxide) ($M_n = 685,000$) was purchased from Polymer Laboratories.

2.1.1. Synthesis of PEO having terminal isocyanato groups (PEO-NCO)

MPEO was reacted with a large excess of hexamethylene diisocyanate (HDI) (5 mol/mol OH), to afford polymer of the formula $MeO(CH_2CH_2O)_nCONH(CH_2)_6NCO$ [24].

2.1.2. Synthesis of two-arm fullerene-containing poly(ethylene oxide) (TAFPEO)

In a three-neck flask, the freshly prepared dry PEO-NCO (2.8 g, 1.3 mmol) was dissolved in 50 ml anhydrous DMF. Fullerenol, $C_{60}(OH)_{10-12}$, (50 mg, 0.65 mmol OH) in DMF (20 ml) was then added dropwise into the PEO-NCO solution in the presence of several drops of dibutyltin dilaurate, as a catalyst. The reaction mixture was stirred at 60 °C under nitrogen for 36 h. At the end of the reaction, unconverted isocyanate functional groups were quenched by the addition of methanol. The solution was evaporated to dryness, and toluene was then added to dissolve the mixture. Unreacted fullerenol which could not dissolve in toluene was filtered off. The reaction product mixture solution was concentrated under a reduced pressure. The removal of the byproduct, which resulted from the reaction of methanol with the uncoverted prepolymer (PEO-NCO), was accomplished by repeated precipitation of products from the toluene solution into hexane, followed by washing with a mixture of toluene and hexane for several times. The final brownish product is soluble in a variety of solvents, such as water, THF, DMF, toluene, etc.

Prior to the isocyanate-hydroxy condensation reaction, the fullerenol was dried under vacuum at 60 °C for 24 h. Complete removal of residual water from the reaction medium was accomplished by further treatment of the fullerenol-containing DMF solution with molecular sieves (4 Å) for at least 2 days.

2.2. Equipment and experiments

2.2.1. FTIR characterization

Infrared spectra were recorded on a Bio-Rad 165 FTIR spectrophotometer. Thirty-two scans were signal-averaged at a resolution of 2 cm^{-1}. The samples (except for PEO-NCO) were prepared by grinding the dry powders with KBr and compressing the mixture to form disks. The disks were stored in a desiccator to avoid moisture absorption. For PEO-NCO, a mixture of nujol and PEO-NCO was placed between a pair of KBr salt windows and eight scans were signal-averaged at a resolution of 1 cm^{-1}. All spectra were recorded at room temperature.

2.2.2. X-ray photoelectron spectroscopic (XPS) measurements

XPS measurements were made on a VG ESCALAB MkII spectrometer with a Mg Kα X-ray source (1253.6 eV photons) and a hemispherical energy analyzer. Various samples were ground to fine powders and then mounted on standard sample studs by means of a double-sided adhesive tape. The X-ray source was run at 12 kV and 10 mA. A pass energy of 20 eV and a rate of 0.05 eV/step were used for all the high-resolution XPS spectra acquisition with a binding energy width of 12 eV. The pressure in the analysis chamber was maintained at 10^{-8} mbar or lower during the measurements. All spectra were obtained at a

take-off angle of 75° and they were curve-fitted with XPSPEAK3.1.

2.2.3. Thermal analysis

DSC measurements were carried out on a TA Instruments 2920 Differential Scanning Calorimeter. The instrument was calibrated with an indium standard and a nitrogen atmosphere (flow rate = 50 ml/min) was used throughout. Samples were first heated to 180 °C and kept at that temperature for 2 min. They were then cooled to −40 °C at a cooling rate of 10 °C/min. After being kept at −40 °C for 2 min, the samples were reheated to 180 °C at 10 °C/min. The melting temperature was obtained from the maximum of the melting endotherm. The degree of crystallinity was determined by comparing the heat of fusion of the sample with that of 100% crystallized PEO (203 J/g) [25].

Thermogravimetric measurements were made with a TA Instruments SDT 2960 Simultaneous DTA-TGA. About 8 mg of sample was heated at 5 °C/min from room temperature to 1000 °C in a dynamic nitrogen atmosphere (flow rate = 50 ml/min).

2.2.4. MALDI-TOF mass spectrometric measurements

Mass spectrometric study was performed using the MALDI-TOF mass spectrometry technique. A Voyager-DE™ spectrometer was used for the positive ion MALDI-TOF experiments. The instrument was equipped with a nitrogen laser (337 nm) and delayed extraction. The detection was operated at an accelerating potential of 25 kV in linear mode. The MALDI mass spectrum represents an average over 100 consecutive laser shots. The MALDI samples were prepared following the published method [26].

2.2.5. GPC measurements

GPC measurements were performed on a Waters system with three Polymerx Polysep-GFC-P linear (300 × 7.8 mm) columns calibrated with PEO standards, a Waters 600E system equipped with a Waters 410 differential refractometer (RI) detector, and a Waters 486 ultraviolet–visible (UV–vis) detector set at 320 nm with deionized H_2O as the eluent. The TAFPEO aqueous solution concentration is about 0.5%.

2.2.6. Laser light scattering measurements

The aggregation behavior of TAFPEO in THF or water solutions was studied by static and dynamic light scattering (DLS) techniques. The measurement concentrations varied from 0.049 to 0.294 mg/ml for aqueous solutions and 0.218 to 0.544 mg/ml for THF solutions. Prior to LLS measurements, all samples were centrifuged at 2.5×10^3 rpm for 2 h to remove dust.

A Brookhaven BI200 goniometer equipped with a BI9000AT digital correlator was used to perform the static and DLS measurements. The light source is a power adjustable argon-ion laser with the wavelength of 488 nm. The measured temperature was controlled at 25 ± 0.1 °C using a Science/Electronic water bath. For SLS, the refractive index increment was measured by a BI-DNDC differential refractometer. For DLS, the inverse Laplace transformation routine based on REPES supplied with the GENDIST software package was used to analyze the time correlation function and the ratio of reject was set to 0.5 [27].

2.2.7. Transmission electron microscopy measurement

TEM micrographs were obtained with a JEOL CX100 operating at an accelerating voltage of 100 kV. For the observation of size and distribution of aggregates, a drop of dilute solution was placed onto a 200 mesh copper grid coated with carbon. The samples were dried before measurement.

3. Results and discussion

3.1. Characterization of TAFPEO

The IR spectrum of PEO-NCO shows the absence of hydroxyl band in the 3480–3550 cm^{-1} region and the presence of a strong IR band at 2272 cm^{-1} for the isocyanate groups (Fig. 1(b)), indicating a complete reaction of the terminal hydroxyl groups of PEO to form PEO-NCO. As shown in Fig. 1(c), the urethane-connected C_{60}-containing PEO shows the absence of the isocyanate band at 2272 cm^{-1}. The conversion of isocyanate groups to urethanes was further evidenced by the appearance of bands at 3330 and 1720 cm^{-1}, corresponding to the urethanic NH and carbonyl absorptions, respectively. A similar conversion of isocyanate has been reported by Chiang and co-workers [21,22]. The spectrum of this C_{60}-based urethane-connected PEO bears a close resemblance to that of MPEO (Fig. 1(a)). Additionally, the infrared absorption of the fullerene moieties in the final product (Fig. 1(c)) was relatively weak in intensity.

XPS is a useful tool for the characterization of C_{60}-containing PEOs [28–30]. Fig. 2 shows the XPS spectrum of TAFPEO. The C1s spectrum shows the existence of two

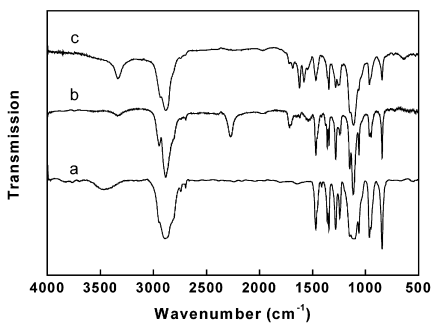

Fig. 1. FTIR spectra of (a) poly(ethylene glycol) monomethyl ether (MPEO); (b) mono-isocyanate terminated PEO (PEO-NCO); (c) two-arm fullerene-containing PEO (TAFPEO).

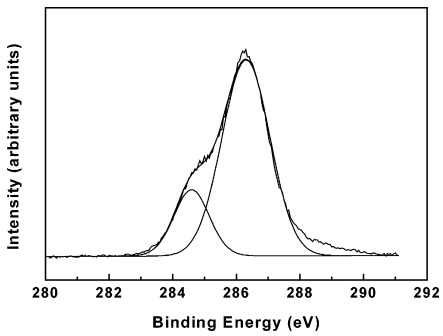

Fig. 2. C1s spectrum of TAFPEO.

different states of carbon. The low-binding-energy peak is centered at 284.6 eV, corresponding to the nonoxygenated carbons of C_{60}. The high-binding-energy peak is centered at 286.4 eV, corresponding to the mono-oxygenated carbon in the PEO chain and fullerenol. The electronegative oxygen makes the mono-oxygenated carbon electron-deficient, leading to a higher binding energy. From peak area measurements, the low-binding-energy peak represents 19.1% of all the carbon, which agrees well with the theoretical value of 19.5% assuming two PEO chains attached to each C_{60} molecule.

The thermogravimetric (TG) curves of pristine C_{60}, MPEO, and TAFPEO are shown in Fig. 3. Pure C_{60} is thermally stable below 600 °C, and PEO decomposes completely above 400 °C. The weight remaining after heating to 600 °C is about 13.1% which is consistent with the theoretical value of 13.4% assuming two-arm PEO chains in the TAFPEO. Therefore, both XPS and TG results suggest that the polymer mainly consists of two PEO chains and can be described as a two-arm C_{60}-containing PEO.

GPC is commonly used for the determination of molecular weight and polydispersity of a polymer. However, GPC, which is based on the variation of hydrodynamic volume of polymers with molecular weights, is affected seriously when the polymers form aggregates. For example, when up to two PEO chains were grafted on C_{60}, the polymer was found to aggregate in THF so that GPC was unable to give its actual molecular weight [19,20]. Similarly, aggregates of TAFPEO in THF, DMF, and water caused difficulties in GPC measurements and this will be discussed later. Based on the same reason, it is a challenging and difficult task to use laser light scattering techniques to determine the molecular weight and molecular weight distribution of single polymer chain. Thus, MALDI-TOF was used to determine the molecular weight of TAFPEO. MALDI-TOF has been increasingly used to determine the average molecular weights of synthetic polymers [31]. Prior to the MALDI-TOF measurement, TAFPEO was purified further by exclusion HPLC in THF with the UV–vis detector set at 320 nm where the PEO is not detected but C_{60} or its derivatives absorb. The presence of C_{60} in TAFPEO was confirmed. Fig. 4 shows the MALDI spectrum for TAFPEO. Its number-average molecular weight ($M_n = 5140$) and polydispersity (1.05) were computed from this spectrum. The presence of one significant peak indicates the TAFPEO sample predominantly consists of C_{60} with two arm PEO chains in a remarkably narrow distribution. The attachment of only two PEO arms on each polyhydroxylated fullerene (fullerenol) molecule may be due to the steric hindrance effect of the bulky fullerene molecule [21,22].

The DSC curves of pristine PEO and TAFPEO are shown in Fig. 5. The crystallization of PEO is greatly affected by the incorporation of C_{60}. The incorporation of C_{60} causes a decrease in the melting temperature from 56.9 to 50.9 °C, and the degree of crystallinity also decreases from 94.2 to 54.8%.

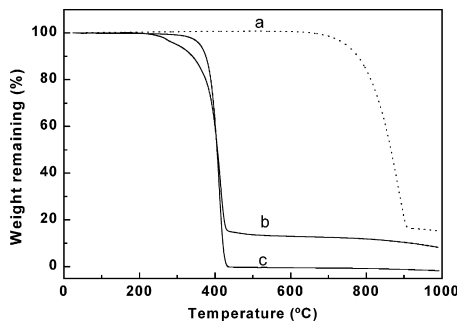

Fig. 3. TGA curves of (a) pristine C60 (dashed line); (b) TAFPEO; (c) MPEO.

3.2. Aggregation of TAFPEO

3.2.1. GPC measurements

It is well established that amphiphilic molecules can associate to form aggregates in aqueous solution [32]. The micellization of various amphiphilic copolymers of PEO in aqueous solutions has been reported [33–35]. Fig. 6 shows the GPC traces of aqueous solutions of TAFPEO, MPEO, and a standard PEO. The two GPC traces of TAFPEO, detected by a UV–vis (at $\lambda = 320$ nm) and an RI detector, respectively, are nearly identical, indicating that fullerene is present in the aggregates of TAFPEO. For TAFPEO, peaks at very short elution times were observed which correspond to an apparent molecular weight of the order 10^6–10^7, compared with that of the standard PEO ($M_n = 685,000$). It

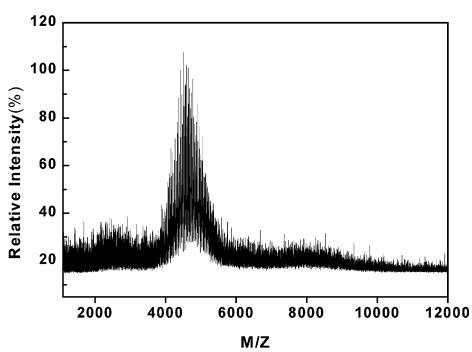

Fig. 4. MALDI-TOF spectrum of TAFPEO.

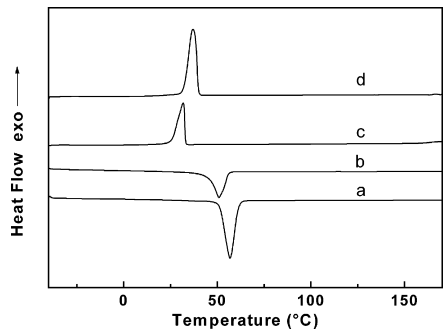

Fig. 5. DSC heating curves of (a) the starting MPEO; (b) TAFPEO, and DSC cooling curves of (c) TAFPEO; (d) the starting MPEO.

is clear that the highly hydrophobic fullerene favors its very large aggregate formation and eliminates the aggregate dissociation, namely, the absence of unimers. The micellization of C_{60}-containing poly(*n*-butyl methacrylate) (FPBMA) involves an equilibrium between unimers and micelles [8]. Therefore, the aggregation of TAFPEO is different from the micellization of FPBMA. The GPC curves of TAFPEO in THF and DMF are too complicated to affirm the existence of the aggregates. The difficulty may be due to the relatively weak interchain association of TAFPEO in THF and DMF so that its aggregation was destroyed to some extent during the elution in the GPC column.

3.2.2. Static light scattering

Both static and dynamic laser light scattering could be used to study the microscopic conformation and the association mechanisms of polymer aggregates in solution [36–39]. For block and graft amphiphilic copolymers based on PEO, their aggregation behaviors and association mechanisms have been extensively investigated by laser light scattering [40–47]. For example, Wu et al. used a combination of static and dynamic laser light scattering to study the self-assemble association of the triblock copolymer of PEO [45].

SLS provides information on the time averaged properties of the system and the weight-average molecular weight (M_w), the second virial coefficient (A_2) and the *z*-average radius of gyration (R_g) based on the relationship

$$\frac{KC}{R_\theta} = \frac{1}{M_w}\left(1 + \frac{q^2R_g^2}{3}\right) + 2A_2C \quad (1)$$

where K ($= 4\pi^2 n_0^2 (dn/dC)^2 / N_A\lambda_0^4$) is an optical constant with N_A, n_0, and λ_0 being the Avogadro's number, the solvent refractive index, and the wavelength of the light in vacuum, respectively. C is the polymer concentration in gram per milliliter and R_θ the excess Rayleigh ratio at scattering angle θ. The scattering vector, q ($= 4\pi n \times \sin(\theta/2)/\lambda$), is defined as the difference of the scattered and the incident beam. The refractive index increment of the polymer solutions, (dn/dC), could be measured using the differential refractometer.

The Zimm plot of TAFPEO in aqueous solutions is shown Fig. 7. It was found that the apparent M_w, A_2 and R_g are 5.53×10^6 g/mol, -1.53×10^{-4} cm^3 mol/g^2 and 117 nm, respectively. It was obvious that the measured M_w is much larger than that obtained from the MALDI-TOF MS measurement, which indicates the existence of large aggregates in solution. At the same time, the SLS data agrees well with the GPC results. The average aggregation number of the TAFPEO in the aqueous solution could be determined from Eq. (2):

$$N_{agg} = \frac{M_w(\text{aggregate})}{M_w(\text{unimer})} \quad (2)$$

It was found that the aggregation number is about 1020. The negative value of the second virial coefficients indicates that water is a poor solvent for TAFPEO.

Fig. 8 shows the Zimm plot of TAFPEO in THF solutions. From the plot, the apparent M_w, A_2 and R_g are 2.94×10^6 g/mol, 4.69×10^{-5} cm^3 mol/g^2 and 131 nm, respectively. The calculated aggregation number of TAFPEO in THF is around 540, which is much smaller than that in aqueous solution. The smaller value of A_2 also suggests that THF is not a good solvent for TAFPEO, however, the solvent quality has improved when compared to water. As a result, the aggregation of TAFPEO in THF is not as significant as that in water.

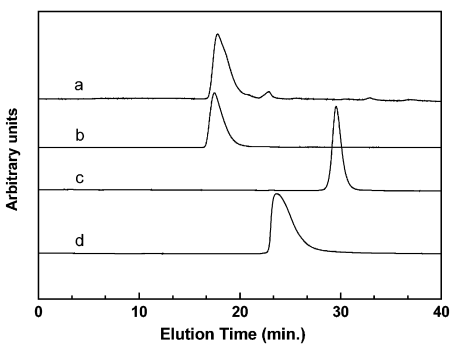

Fig. 6. GPC traces of TAFPEO (a) RI detector; (b) UV detector; and the starting MPEO (c) RI detector; and the standard PEO (d) RI detector.

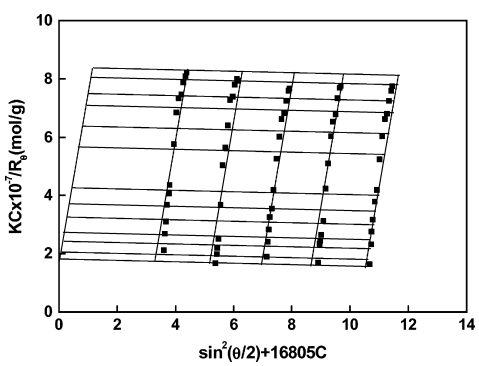

Fig. 7. Zimm plot of TAFPEO in water, where $T = 25$ °C and the polymer concentration ranged from 0.049 to 0.294 mg/ml.

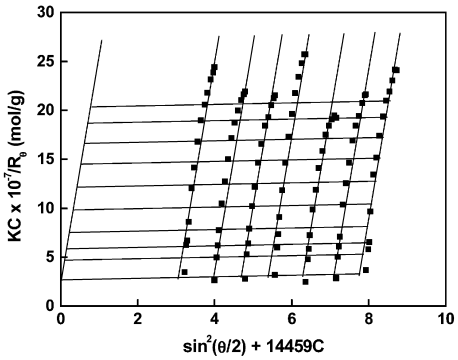

Fig. 8. Zimm plot of TAFPEO in THF, where $T = 25$ °C and the polymer concentration ranged from 0.218 to 0.544 mg/ml.

3.2.3. Dynamic light scattering

DLS measures the temporal fluctuations of the scattered light produced by the Brownian diffusion of polymer molecules. The intensity of the scattered lights was analyzed by the photon correlation spectroscopy (PCS) [48,49]. The normalized field autocorrelation function is described by the expression

$$g_1(t) = \int w(\Gamma)\exp(-\Gamma t)\mathrm{d}\Gamma \tag{3}$$

where $w(\Gamma)$ is a continuous distribution function of decay rate Γ, which is the inverse of the decay time τ. If the inverse Laplace transform (ILT) is used to analyze the autocorrelation function, the decay time distribution function can be obtained. For the translational diffusion mode, the translational diffusion coefficient D is related to the decay rate by the expression when the measurement angle θ is close to 0:

$$D = \frac{\Gamma}{q^2} \tag{4}$$

Fig. 9 shows the decay time distribution of 0.272 mg/ml TAFPEO in THF at different measurement angles. It is evident that only a single peak is present in the distribution function, which indicates that the TAFPEO aggregates are present in the solution. However, the peak is not narrow, suggesting that the size distribution of the aggregates is

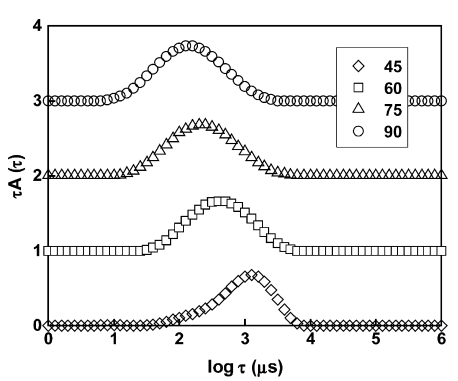

Fig. 9. Decay time distribution function of the typical THF solution of TAFPEO of 0.272 mg/ml, at 25 °C.

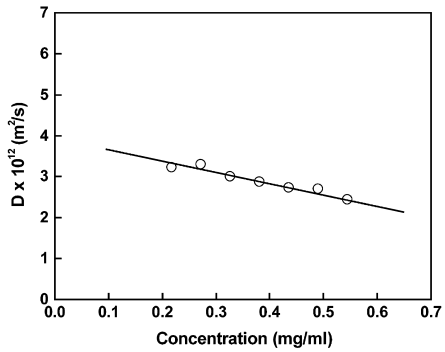

Fig. 10. Concentration dependence of diffusion coefficients for TAFPEO in THF solutions at 25 °C.

broad. This can also be observed in the TEM micrographs described in Section 3.2.4.

The concentration dependence of diffusion coefficients for TAFPEO in THF solutions is shown in Fig. 10. A linear relationship is observed with an intercept of 3.85×10^{-12} m^2/s, which corresponds to the diffusion coefficient D_0 of TAFPEO in infinitely dilute solution. From the Stokes–Einstein equation, the hydrodynamic radius, R_h, can be determined from

$$R_h = \frac{kT}{6\pi\eta_0 D_0} \tag{5}$$

where k is the Boltzmann constant, T the absolute temperature in Kelvin, η_0 the solvent viscosity. It was found that R_h is 123 nm and the value of R_g/R_h equals 1.06, which indicates a hard sphere structure for TAFPEO in THF solutions. The negative slope corresponds to the diffusion virial coefficients.

Since the R_g value of TAFPEO in THF is reasonably large (>100 nm), the size of the aggregate in a more polar solvent such as water would be even bigger. In order to determine the large aggregate in water, the measurements must be performed at smaller measurement angles such that $(qR_g) < 1$–2. This is usually very difficult for systems in aqueous environment due the anomalous scattering from dust at small angles. Thus the absolute value of R_h in water cannot be determined with confidence. However, by comparing the SLS data on A_2, R_g and N_{agg}, it is believed that TAFPEO has a more compact structure in water than in THF.

3.2.4. Transmission electron microscopy measurement

TEM has been used as a reliable technique to determine the micelle formation of polymers in solution [50], and to demonstrate the aggregation of C_{60} or C_{60} derivatives [51–54]. The aggregation of TAFPEO in water, THF, or DMF was confirmed by TEM using dried sample obtained from dilute solutions. The TEM micrographs of TAFPEO aggregates are shown in Fig. 11. It can be observed that the samples consist of isolated spherical clusters with an average diameter of 210, 80, and 90 nm, for samples obtained from dilute aqueous, THF, and DMF solution,

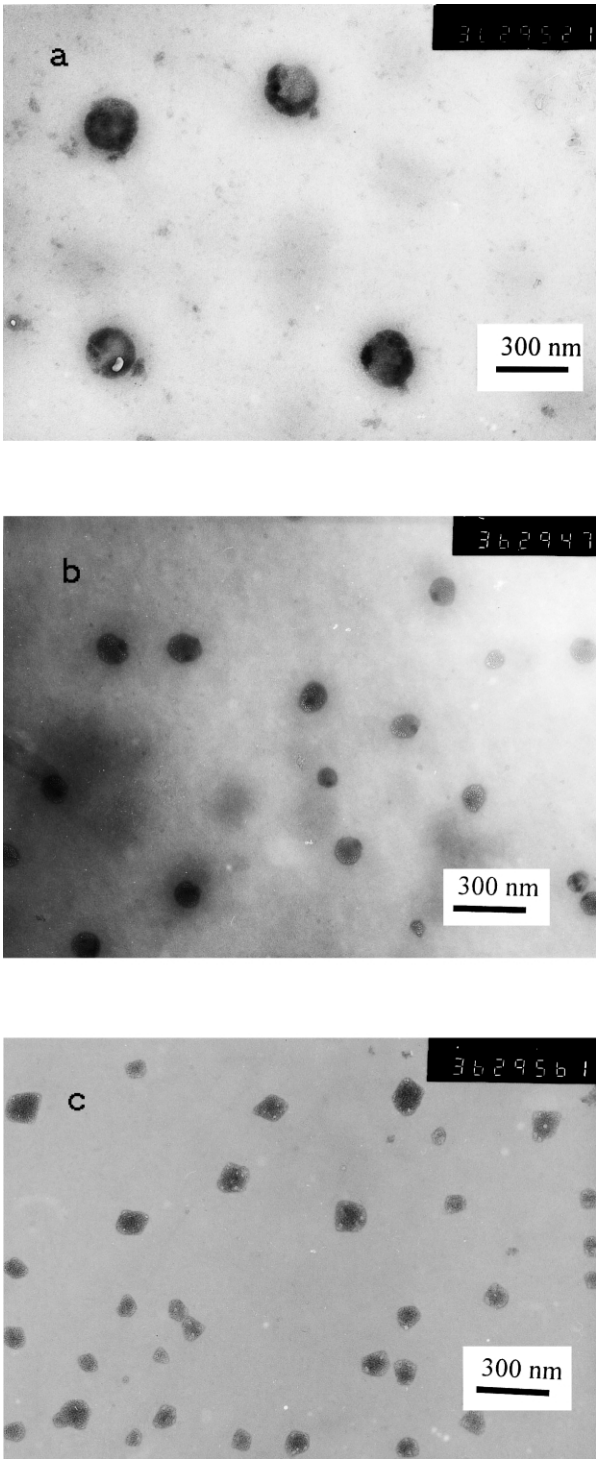

Fig. 11. Typical transmission electron micrographs of aggregates prepared from TAFPEO in water (a), in THF (b), and in DMF (c).

respectively. In general, the apparent hydrodynamic diameters are larger than the TEM diameters because dynamic LLS gives the size of the solvent-swollen aggregates and TEM gives the size of dry particles. Furthermore, TEM gives the size of the C_{60} portion only and dynamic LLS measures the size of the whole sphere.

We have also studied the aggregation behavior of single-C_{60}-end-capped PEO (FPEO) and double-C_{60}-end-capped PEO (FPEOF) [55]. The chain length of PEO in FPEO ($M_n = 2200$) is about the same as that in TAFPEO ($M_n = 2050$), whereas the chain length of PEO in FPEOF is longer ($M_n = 5000$). The aggregation numbers of FPEO and FPEOF in THF are 13,800 and 1320, respectively [55]. Therefore, the architecture of the C_{60}-containing PEO plays an important role on its aggregation behavior.

4. Conclusion

A water-soluble fullerene-containing poly(ethylene oxide) (PEO) predominantly with two PEO chains was synthesized through isocyanate-hydroxy condensation reaction, utilizing fullerenol as a molecular core. The presence of C_{60} causes the amphiphilic polymer to form very large spherical aggregates in polar solvents, such as water, THF, and DMF, with an aggregation number around 540–1020. In comparison, for PEO hydrophobically modified by *n*-hexadecyl group, the aggregation number in water is around 40–90 [56]. Therefore, the stronger hydrophobicity of C_{60} leads to a greater extent of aggregation.

Acknowledgements

We thank Mr H.K. Wong for assistance in XPS measurements and Ms X.H. Wang for assistance in MALDI-TOF measurements.

References

[1] For recent reviews on fullerene chemistry see: (a) Jensen AW, Wilson SR, Schuster DI. Bioorg Med Chem 1996;4:767. (b) Prato M. J Mater Chem 1997;7:1097. (c) Karaulova EN, Bagrii EI. Russ Chem Rev 1999;68:889. (d) Diederich F, Gomez-Lopez M. Chem Soc Rev 1999; 28:263.
[2] Weis C, Friedrich C, Mulhaupt R, Frey H. Macromolecules 1995;28: 403.
[3] Sun YP, Ma B, Bunker CE, Liu B. J Am Chem Soc 1995;117:12705.
[4] Okamura H, Terauchi T, Minoda M, Fukuda T, Komatsu K. Macromolecules 1997;30:5279.
[5] Okamura H, Ide N, Minoda M, Komatsu K, Fukuda T. Macromolecules 1998;31:1859.
[6] Okamura H, Minoda M, Fukuda T, Miyamoto T, Komatsu K. Macromol Rapid Commun 1999;20:37.
[7] Lu ZH, Goh SH, Lee SY. Polym Bull 1997;39:661.
[8] Wang XH, Goh SH, Lu ZH, Lee SY, Wu C. Macromolecules 1999;32: 2786.
[9] Weber V, Duval M, Ederlé Y, Mathis C. Carbon 1998;36:839.
[10] Li CZ, Zhang WC, Zhou P, Du FS, Li ZC, Li FM, Du FS. Acta Polym Sin 2001;4:557.
[11] Zhou SQ, Burger C, Chu B, Sawamura M, Nagahama N, Toganoh M, Hackeler UE, Isobe H, Nakamura E. Science 2001;291:1944.
[12] Samal S, Geckeler KE. Chem Commun 2001;2224.
[13] Angelini G, Maria PD, Fontana A, Pierini M, Maggini M, Gasparrini F, Giovanni Z. Langmuir 2001;17:6404.

[14] Hawker CJ, Saville PM, White JW. J Org Chem 1994;59:3503.
[15] Delpeux S, Beguin F, Benoit R, Erre R, Manolova N, Rashkov I. Eur Polym J 1998;34:905.
[16] Huang XD, Goh SH, Lee SY. Macromol Chem Phys 2000;201:2660.
[17] Manolova N, Rashkov I, Begiun F, Damme HV. Chem Commun 1993;1725.
[18] Delpeux S, Béguin F, Manolova N, Rashkov I. Eur Polym J 1999;35:1619.
[19] Ederlé Y, Mathis C, Nuffer R. Synth Met 1997;86:2287.
[20] Ederlé Y, Mathis C. Fullerene Sci Technol 1996;4:1177.
[21] Chiang LY, Wang LY, Tseng SM, Wu JS, Hsieh KH. J Chem Soc, Chem Commun 1994;2675.
[22] Chiang LY, Wang LY, Kuo CS. Macromolecules 1995;28:7574.
[23] Chiang LY, Wang LY, Swirczewski JW, Soled S, Cameron S. J Org Chem 1994;59:3960.
[24] Zalipsky S, Gilon C, Zilkha A. Eur Polym J 1983;19:1177.
[25] Wuderilich B, Macromolecular physics, vol. 3. New York: Academic Press; 1980.
[26] Montaudo G, Montaudo MS, Pulglisi C, Samperi F. Macromolecules 1995;28:4562.
[27] Jakes J. Czech J Phys B 1988;38:1305.
[28] Huang XD, Goh SH, Lee SY. Macromol Chem Phys 2000;201:2660.
[29] Huang XD, Goh SH. Macromolecules 2000;33:8894.
[30] Song T, Goh SH, Lee SY. Macromolecules 2002;35:4133.
[31] Hanton SD. Chem Rev 2001;101:527.
[32] Lindman B, Wennerström H. Top Curr Chem 1980;87:1.
[33] Patrickios CS, Forder C, Armes SP, Billingham NC. J Polym Sci, Part A: Polym Chem 1996;34:1529.
[34] Berlinova VI, Amzil A, Vladimirov NG. J Polym Sci, Part A: Polym Chem 1995;33:1751.
[35] Wesslén B, Wesslén KB. J Polym Sci, Part A: Polym Chem 1992;30:355.
[36] Dai S, Tam KC, Jenkins RD. Macromolecules 2000;33:404.
[37] Dai S, Tam KC, Jenkins RD, Bassett DR. Macromolecules 2000;33:7021.
[38] Dai S, Tam KC, Jenkins RD. Macromolecules 2001;34:4673.
[39] Dai S, Tam KC, Jenkins RD. Macromol Chem Phys 2001;202:335.
[40] Qiu XP, Wu C. Macromolecules 1997;30:7921.
[41] Wu C, Qiu XP. Phys Rev Lett 1998;80:620.
[42] Hu TJ, Wu C. Phys Rev Lett 1999;83:4105.
[43] Gan ZH, Jim TF, Li M, Yuez Z, Wang S, Wu C. Macromolecules 1999;32:590.
[44] Wu C, Fu J, Zhao Y. Macromolecules 2000;33:9040.
[45] Zhao Y, Liang H, Wang S, Wu C. J Phys Chem B 2001;105:848.
[46] Dai S, Tam KC, Jenkins RD. J Phys Chem B 2001;105:10189.
[47] Gourier C, Beaudoin E, Duval M, Sarazin D, Maître S, François J. J Colloid Interf Sci 2000;230:41.
[48] Chu B. Laser light scattering—basic principles and practice, 2nd ed. Boston: Academic Press; 1991.
[49] Brown W. Dynamic light scattering—the method and some applications. Boston: Clarendon Press; 1991.
[50] Báñez MV, Robinson KL, Vamvakaki M, Lascelles SF, Armes SP. Polymer 2000;41:8501.
[51] Cassell AM, Asplund CL, Tour JM. Angew Chem Int Ed 1999;38:2403.
[52] Mendoza D, Gonzalez G, Escudero R. Adv Mater 1999;11:31.
[53] Ouyang JY, Goh SH, Li Y. Chem Phys Lett 2001;347:344.
[54] Yang CY, Heeger AJ. Synth Met 1996;83:85.
[55] Song T, Dai S, Tam KC, Lee SY, Goh SH. submitted to Langmuir.
[56] Beaudoin E, Borisov O, Lapp A, Billon L, Hiorns RC, François J. Macromolecules 2002;35:7436.